# Development of a quick-stop device for micro-cutting

Romain Piquard[1] · Alain D'Acunto[1] · Michaël Fontaine[2] · Sébastien Thibaud[2] · Alexandre Gilbin[2] · Gaël Le Coz[1]

**Abstract**
Micro-cutting is characterised by undeformed chip thicknesses in the micron range. This range leaves little choice of in situ observation techniques. One solution is therefore to observe these zones a posteriori after the cutting has been abruptly interrupted. This technique has proven to be very useful for conventional machining. This paper deals with the development of a quick-stop device dedicated to micro-cutting. The aim of this device is to observe cutting mechanisms and chip formation at this scale in order to enhance micro-cutting models.

**Keywords** Micro-cutting · Quick-stop device · Chip formation · Machining

## 1 Introduction

Micro-machining by material removal, has been widely developed due to its versatility in terms of machinable material and the geometry of the part that can be produced. For exemple, micro-milling can be found in various industrial fields (mechanical, electronic, luxury goods, medical, etc.) for the machining of a wide range of materials [1]. The main axis of development has been to adapt conventional machining to a smaller scale, in the micron range. However, this approach has shown its limits due to the appearance of scale effects, corresponding to a divergence of certain parameters during homotheticity. The order of magnitude of the microstructure of the machined material and the tool material is, for example, close to the order of magnitude of the cutting parameters. These scale effects then tend to lead to tool-material interaction and chip formation specific to micro-machining [2]. Unlike conventional scale, micro-machining is largely influenced by the slightest disturbance such as run-out, deflection or material heterogeneity. The investigation of micro-cutting is then necessary to study these phenomena. A first approach consists in cutting force measurements in a simple con uration such as orthogonal cutting [3].

Another means of investigation to identify local phenomena is to abruptly interrupt the cut to freeze and then observe the formation of the chip by suitable means (SEM, EDX, EBSD) in order to confirm hypotheses [4]. This technique, which has been tried and tested on a conventional scale, is rare on a micro-machining scale. However, these systems are complex to create so that the cutting process is disturbed as little as possible. This work thus proposes a quick-stop device adapted to micro-machining.

In her thesis Rebaioli [5] did an exhaustive state-of-the-art review about quick-stop devices. A classification was proposed (Fig. 1) and the conclusion is that most devices work on the same principle: the cutting speed is obtained by rotation of the workpiece and the interruption of the cut is obtained by acceleration of the tool. The triggering system works on the principle of breakage of a shear pin by

✉ Romain Piquard
romain.piquard@univ-lorraine.fr

Alain D'Acunto
alain.dacunto@ensam.eu

Michaël Fontaine
michael.fontaine@femto-st.fr

Sébastien Thibaud
sebastien.thibaud@femto-st.fr

Alexandre Gilbin
alexandre.gilbin@ens2m.fr

Gaël Le Coz
gael.lecoz@univ-lorraine.fr

[1] Department T-PRIOM, LEM3 UMR CNRS 7239, 7 rue Félix Savart, Metz 57070, France

[2] Department of Applied Mechanics, FEMTO-ST UMR CNRS 6174, 24 rue de l'épitaphe, Besançon 25000, France

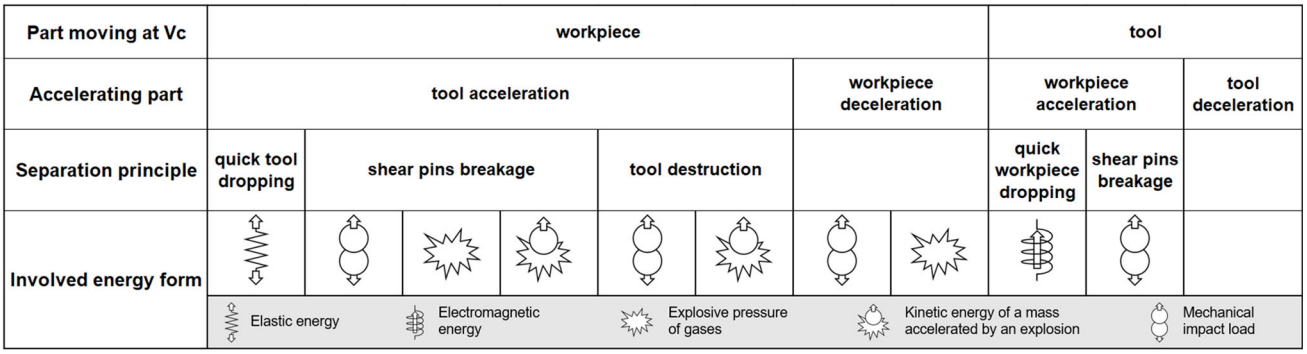


**Fig. 1** Classification of QSD adapted from [5]

mechanical load impact, as those developed in [6, 7]. The constraints for designing a quick-stop device are as follows:

- an ejection speed higher than the cutting speed,
- a short separation time to limit the influence on chip formation,
- a direction of ejection adapted to cutting parameters to prevent sliding of clearance face on previously machined surface,
- sufficient rigidity to minimise disruption of the cut during interruption.

However, quick-stop devices dedicated to micro-cutting are rare. Only two are mentioned in the literature.

Rebaioli developed a quick-stop device using a glass shear pin to hold the tool holder and a percussion system using expansion of pressurized air to accelerate the striker. The separation time is between 55 and 75 $\mu$s and separation distance of about 50 $\mu$m for a cutting speed of 100 m/min. The device was tested for an uncut chip thickness of 50 $\mu$m.

The second one was developed by Schneider et al. [8, 9]. The separation is provided by the abrupt release of a pre-loaded spring attached to the tool holder. The release is obtained by retraction of a pin due to expansion of pressurized air controlled by a magnetic valve. There is no indication of device characteristics but the cutting speed used in experimentation of 1.1 m/min was quite low to consider low separation time and distance. The uncut chip thickness was set up between 0.4 and 10 $\mu$m.

Subbiah and Melkote [10] as well as Uysal and Altan [11] investigated the effect the cutting edge radius on chip formation and cutting forces using a quick-stop device but the uncut chip thickness was above 15 $\mu$m for the first one and above 100 $\mu$m for the second one, that is over the consideration in this work.

In this work, a quick-stop device is developed in order to reach usual uncut chip thickness and cutting speed values in micro-milling or micro-turning.

## 2 Method

### 2.1 Device principle

In the context of micro-cutting, the cutting forces are of the order of 10N due to uncut chip thicknesses less than 10 $\mu$m. The cutting speed is also limited: in micro-milling, a spindle speed of 60,000 rev/min for a micro-end-mill of 0.5 mm diameter gives a cutting speed of less than 100 m/min. A classical device using explosive pressure and shear pins would be oversized. The design was therefore oriented towards a system dedicated to micro-cutting, for use on a milling centre, thus providing a larger working area as the cutting force measurement device presented in [3]. The quick-stop device for micro-cutting consists of a spring-loaded projectile and a translatory part containing the tool (Fig. 2).

The mobile carriage is arranged on two ball rails, thus providing a high degree of rigidity. These rails are screwed on a 15° inclined plane. In micro-cutting an elastic recovery due to cutting edge radius occurs. In this way, to avoid tool slip on machined surface with the clearance face, the extraction direction has to be greater than clearance angle. An angle two times greater than clearance angle (7°) has been chosen. The traditional mechanical fuse system is replaced here by a magnetic fuse. A permanent neodymium magnet capable of exerting a maximum force of 140 N is used to hold the moving part. As the magnetic forces of a permanent magnet result from edge effects, it has not been possible to define the theoretical force of attraction on contact, but tests have allowed an experimental estimate of the magnet's force of attraction of the order of 35N. As the impact force is greater than the magnet's attraction force, the latter is sufficient to detach the moving part and release it from the machining area.

The striker consists of a movable cylinder in a body by a loaded spring. The piston is locked by a shaft with a flattened surface. The rotation of this shaft with the trigger releases the cylinder which moves under the action of the spring (Fig. 3a). Once the piston has reached its maximum speed, it strikes the

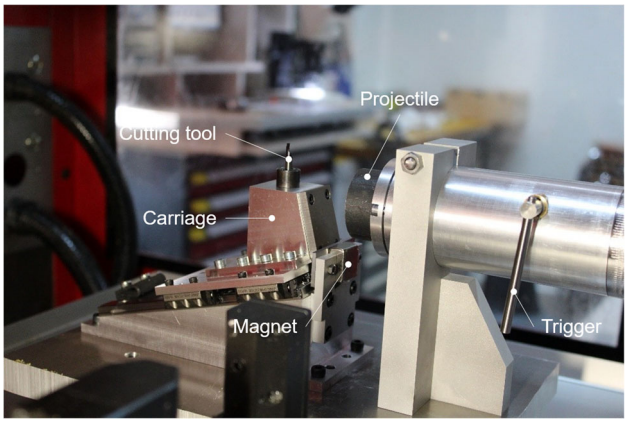


**Fig. 2** Quick-stop device

carriage (Fig. 3b) which in turn moves in the defined direction (Fig. 3c). Once the carriage has reached the end of its travel and the test is completed, the system is reassembled by unscrewing the cover, allowing the cylinder to retract freely and re-lock. The spring is then compressed by closing the cover and the carriage can be returned to its original position.

The striker is an important part of the QSD. Due to its inertia, the cylinder first allows the fuse system to break and then defines the speed of the tool ejection.

## 2.2 Impact study

The selection of the impact system was based on simplicity and low cost of manufacture and no use of consumables. A piston system with a compressed spring released by a trigger was preferred to the traditional gas or bullet system. Thus, the speed of ejection is given by the energy released when the spring is released. The use of a bronze ring with a graphite bushing makes it possible to assume that the piston is not subject to any (negligible) friction. According to this assumption, the elastic energy is therefore entirely transformed into kinetic energy.

$$\frac{1}{2}K(l-l_0)^2 = \frac{1}{2}m_1V^2 \tag{1}$$

where $K$ is the stiffness of the spring propelling the striker, $l$ its length after compression, $l_0$ the no-load length, $m_1$ the mass of the piston, and $V$ its velocity after expansion.

The component of the velocity of the piston at the end of the stroke on the axis of clearance of the mobile carriage can then be deduced with $a_d$ the angle of disengagement of the carriage, corresponding to the speed before impact, noted $V_a$.

$$V_a = \sqrt{\frac{K}{m_1}}(l-l_0) \times \cos a_d \tag{2}$$

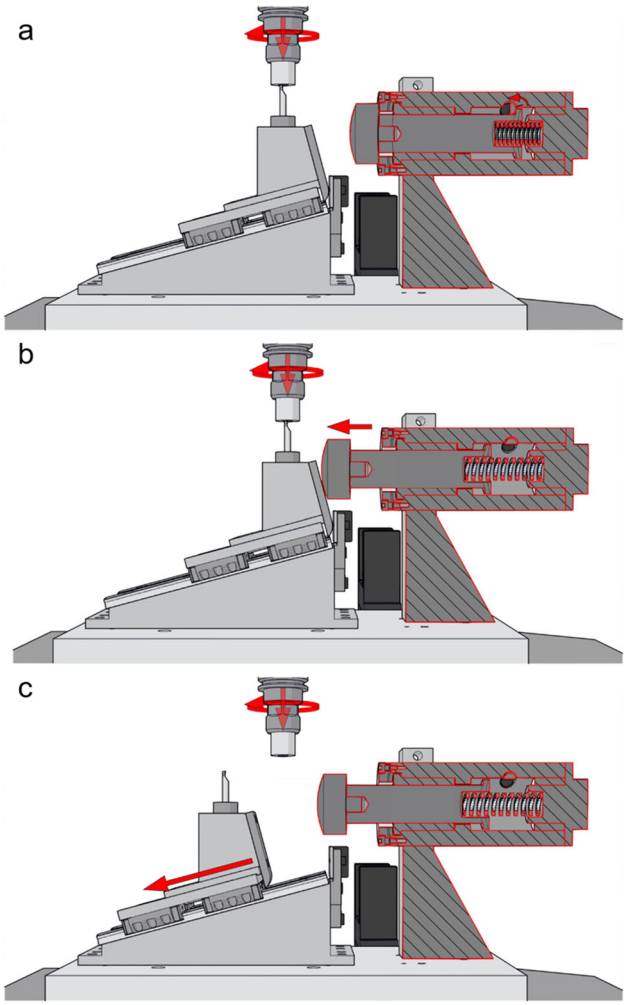


**Fig. 3** Quick stop device principle

In order to identify the parameters needed for the design, the movement between two points in time must also be studied $t_1$ and $t_2$ before and after the impact respectively. Let us consider the part to be chased of mass $m$ as our studied system $\Sigma$ in the galilean reference frame $R_g$. The application of the fundamental principle of dynamics is given by the Eq. 3 and integrating this equality between the two moments gives Eqs. 4 and 5.

$$\left\{ \begin{array}{c} m\vec{\Gamma}(t, G/R_g) \\ \vec{\delta}(t, G/R_g) \end{array} \right\}_G = \left\{ \begin{array}{c} \vec{R}(\bar{\Sigma}/\Sigma) \\ \vec{M}(G, \bar{\Sigma}/\Sigma) \end{array} \right\}_G \tag{3}$$

$$\left\{ \begin{array}{c} \int_{t_1}^{t_2} m\vec{\Gamma}(t, G/R_g)dt \\ \int_{t_1}^{t_2} \vec{\delta}(t, G/R_g)dt \end{array} \right\}_G = \left\{ \begin{array}{c} \int_{t_1}^{t_2} \vec{R}(\bar{\Sigma}/\Sigma)dt \\ \int_{t_1}^{t_2} \vec{M}(G, \bar{\Sigma}/\Sigma)dt \end{array} \right\}_G \tag{4}$$

Thus, when the time interval between the two instants tends to 0, i.e., when $t_1$ tends to $t_-$ and $t_2$ tends to $t_+$ which are the lower and upper limits of the instant $t$ of the impact, we obtain equality between the discontinuity of the kinetic

torsor of the system and the torsor of the external impacts applied to the system.

$$\left\{ \begin{array}{l} m\vec{V}\left(t_2, G/R_g\right) - m\vec{V}(t_1, G/R_g) \\ m\vec{\sigma}\left(t_2, G/R_g\right) - m\vec{\sigma}(t_1, G/R_g) \end{array} \right\}_G = \left\{ \begin{array}{c} \int_{t_1}^{t_2} \vec{R}(\bar{\Sigma}/\Sigma)dt \\ \int_{t_1}^{t_2} \vec{M}(G, \bar{\Sigma}/\Sigma)dt \end{array} \right\}_G \quad (5)$$

$$\left\{ \begin{array}{l} [[m\vec{V}\left(t, G/R_g\right)]] \\ \left[\left[m\vec{\sigma}\left(t, G/R_g\right)\right]\right] \end{array} \right\}_G = \left\{ \begin{array}{c} \vec{P} = \int_{t_-}^{t_+} \vec{R}(\bar{\Sigma}/\Sigma)dt \\ K(\vec{G}) = \int_{t_-}^{t_+} \vec{M}(G, \bar{\Sigma}/\Sigma)dt \end{array} \right\}_G \quad (6)$$

We can apply the fundamental principle of shocks to our two solids in percussion. Let us note $S_1$ the projectile of mass $m_1$ and $S_2$ the moving carriage containing the tool of mass $m_2$.

$$\left\{ \begin{array}{l} [[m_1\vec{V}\left(t, S_1/R_g\right]]) \\ \left[\left[m_1\vec{\sigma}\left(t, S_1/R_g\right)\right]\right] \end{array} \right\}_G = \left\{ \begin{array}{c} \vec{P}_1 = \int_{t_-}^{t_+} \vec{R}(\bar{S_1}/S_1)dt \\ K(\vec{G}) = \int_{t_-}^{t_+} \vec{M}(G, \bar{S_1}/S_1)dt \end{array} \right\}_G \quad (7)$$

$$\left\{ \begin{array}{l} [[m_2\vec{V}\left(t, S_2/R_g\right]]) \\ \left[\left[m_2\vec{\sigma}\left(t, S_2/R_g\right)\right]\right] \end{array} \right\}_G = \left\{ \begin{array}{c} \vec{P}_2 = \int_{t_-}^{t_+} \vec{R}(\bar{S_2}/S_2)dt \\ K(\vec{G}) = \int_{t_-}^{t_+} \vec{M}(G, \bar{S_2}/S_2)dt \end{array} \right\}_G \quad (8)$$

As the magnetic force is bounded during impact, as well as the cutting force, only the impact between the two solids is considered in the impact torsor.

$$\vec{P}_1 = \int_{t_-}^{t_+} \vec{R}(\bar{S_1}/S_1)dt = \int_{t_-}^{t_+} \vec{R}(S_2/S_1)dt \quad (9)$$

$$\vec{P}_2 = \int_{t_-}^{t_+} \vec{R}(\bar{S_2}/S_2)dt = \int_{t_-}^{t_+} \vec{R}(S_1/S_2)dt = -\vec{P}_1 \quad (10)$$

Equations 7, 8, and 10 give the relationship between the speeds in Eq. 11.

$$m_1\vec{V}\left(t_+, S_1/R_g\right) - m_1\vec{V}\left(t_-, S_1/R_g\right) = m_2\vec{V}\left(t_-, S_2/R_g\right) - m_2\vec{V}(t_+, S_2/R_g) \quad (11)$$

A kinematic relationship (Eq. 12) also links the velocities of the point of impact $I$ at the two instants surrounding the impact. This relationship reflects the fact that before the impact the two solids move towards each other and then away from each other.

$$\vec{n_{21}}.\vec{V}\left(t_+,\ I \in S_2/S_1\right) = -e_c\ \vec{n_{21}}.\vec{V}\left(t_-,\ I \in S_2/S_1\right) \quad (12)$$

The coefficient $e_c$ is a coefficient between 0 and 1 depending on the dissipation of kinetic energy during the impact. Here, we will assume a perfectly elastic contact with no friction leading to a coefficient equal to 1.

$$V\left(t_+, S_2/R\right) = V\left(t_-, S_2/R\right) + 2\frac{\left(V\left(t_-, S_1/R\right) - V\left(t_-, S_2/R\right)\right)}{1 + \left(\frac{m_2}{m_1}\right)} \quad (13)$$

$$V\left(t_+, S_1/R\right) = V\left(t_-, S_1/R\right) - 2\frac{\left(V\left(t_-, S_1/R\right) - V\left(t_-, S_2/R\right)\right)}{1 + \left(\frac{m_1}{m_2}\right)} \quad (14)$$

The lower the ratio between the mass of the impacted system and the mass of the projectile, the higher the ejection speed. This has been taken into account in the design, by using aluminium components as much as possible and only one hardened steel plate as a martyr plate during the impact and as a fuse with the magnet. It should be noted that the magnetic attraction force of the magnet is not involved in the study of percussion. In fact, it comes into play in the phase following percussion, when the carriage moves away from the magnet (exponential decrease of the magnetic attraction). The same applies to friction with the guide rails.

Knowing the maximum speed and the mass of the machining system, and by setting the values of the projectile characteristics, the standard spring references can be found to obtain the right ejection speed. By selecting the correct spring, the design of the striker could be finalised. As the supplier has several stiffnesses available, it is possible to obtain several ejection speeds.

### 2.3 Determination of impact duration

On the other hand, the approach presented currently only gives the velocities before and after the impact and does not give any information on the shock itself. The duration of percussion is however as essential as the ejection speed. To know this duration, it is necessary to consider the two elements as elastic and thus study the distance between the centres of gravity during the contact. According to the work of Hertz on the contact between a sphere and a plane, it is possible to link the penetration $\delta$ of the sphere of radius $r$ in the plane subjected to a force $F$. The force is equivalent to the force of

a non-linear spring of stiffness $k$.

$$F = \frac{4E^* r^{\frac{1}{2}}}{3}\delta^{\frac{3}{2}} = k\delta^{\frac{3}{2}} \tag{15}$$

where,

$$E^* = \frac{E}{1-\nu^2} \tag{16}$$

$E^*$ is the Young's modulus renormalized from the Poisson's ratio $\nu$ of the material composing the plane.

By applying the fundamental principle of dynamics to the two solids, a non-linear differential equation is obtained from the difference of the two equations relating relative acceleration $\Gamma$ between the two solids and penetration

$$m_2\Gamma\left(t, S_2/R_g\right) = k\delta^{\frac{3}{2}} \tag{17}$$

$$m_1\Gamma\left(t, S_1/R_g\right) = -k\delta^{\frac{3}{2}} \tag{18}$$

$$\ddot{\delta} + \left(\frac{1}{m_1} + \frac{1}{m_2}\right) k\delta^{\frac{3}{2}} = 0 \tag{19}$$

By multiplying this differential equation by the velocity $\dot{\delta}$, it can be integrated to obtain an equation linking velocity and displacement representing the conservation of enrgy between kinetic and elastic energy.

$$\frac{\dot{\delta}^2}{2} + \left(\frac{1}{m_1} + \frac{1}{m_2}\right)\frac{2}{5} k\delta^{\frac{5}{2}} = cste \tag{20}$$

The constant is obtained when at the end of the impact the penetration is zero ($t = t_+$), the relative velocity between the two parts in contact is given by Eqs. 13 and 14. The differential equation is then completely defined and is given by Eq. 23.

$$\text{At } t = t_+ \ \delta = 0 \text{ and } \dot{\delta} = V\left(t_+, S_2/R\right) - V\left(t_+, S_1/R\right) \tag{21}$$

$$\frac{\dot{\delta}^2}{2} = cste \tag{22}$$

$$\frac{\dot{\delta}^2}{2} + \left(\frac{1}{m_1} + \frac{1}{m_2}\right)\frac{2}{5} k\delta^{\frac{5}{2}} = \frac{1}{2}\left(V\left(t_+, S_2/R\right) - V\left(t_+, S_1/R\right)\right)^2 \tag{23}$$

The maximum penetration $\delta_{max}$, corresponding to the cancellation of the relative speed, can be deduced and is given by Eq. 24. This value also gives with Eq. 19 the maximum relative acceleration $\ddot{\delta}_{max}$ at maximum penetration (Eq. 25).

$$\delta_{max} = \left[\frac{5m_1m_2}{4k\left(m_1+m_2\right)}\left(V\left(t_+, S_2/R\right) - V\left(t_+, S_1/R\right)\right)^2\right]^{\frac{2}{5}} \tag{24}$$

$$\ddot{\delta}_{max} = -\frac{k\left(m_1+m_2\right)}{m_1m_2}\delta_{max}^{\frac{3}{2}} \tag{25}$$

The nondimensionalisation of Eq. 23 by dividing the penetration by the maximum penetration gives an equation to express the time interval $dt$ as a function of the dimensionless penetration $\Delta$ of the two solids.

$$\Delta = \frac{\delta}{\delta_{max}} \tag{26}$$

$$\frac{\delta_{max}^2}{2}\dot{\Delta}^2 + \frac{\left(V\left(t_+, S_2/R\right) - V\left(t_+, S_1/R\right)\right)^2}{2}\Delta^{\frac{5}{2}} = \frac{\left(V\left(t_+, S_2/R\right) - V\left(t_+, S_1/R\right)\right)^2}{2} \tag{27}$$

$$\frac{d\Delta}{dt} = \frac{\left(V\left(t_+, S_2/R\right) - V\left(t_+, S_1/R\right)\right)}{\delta_{max}} \times \sqrt{1-\Delta^{\frac{5}{2}}} \tag{28}$$

$$dt = \frac{\delta_{max}}{\left(V\left(t_+, S_2/R\right) - V\left(t_+, S_1/R\right)\right)} \times \frac{d\Delta}{\sqrt{1-\Delta^{\frac{5}{2}}}} \tag{29}$$

By integrating this equation between $t_-$ and $t^*$ corresponding to the instants when the penetration is zero and is maximum (Eq. 30), and doing the same between $t_{max}$ and

**Table 1** QSD characteristics

| **Inputs** | | | | | | |
|---|---|---|---|---|---|---|
| $K$ | $a_d$ | $l - l_0$ | $m_1$ | $m_2$ | $E^*$ | $r$ |
| 26.44 kN/m | 15 ° | 19.1 mm | 485 g | 605 g | 220 GPa | 40 mm |
| **Outputs** | | | | | | |
| $V\left(t_-, S_1/R\right)$ | $V\left(t_+, S_2/R\right)$ | $\ddot{\delta}_{max}$ | $t_+ - t_-$ | | | |
| 258 m/min | 230 m/min | $109.5\times10^3$ m/s$^2$ | 70 $\mu$s | | | |

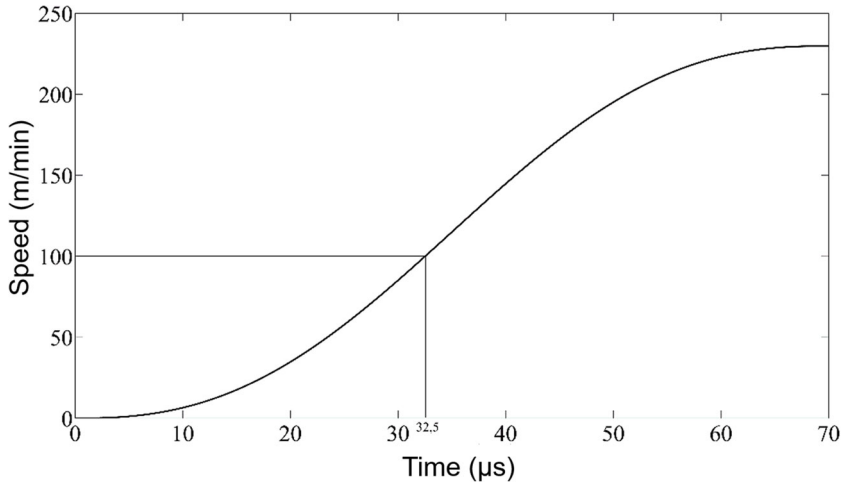


**Fig. 4** Carriage speed during separation

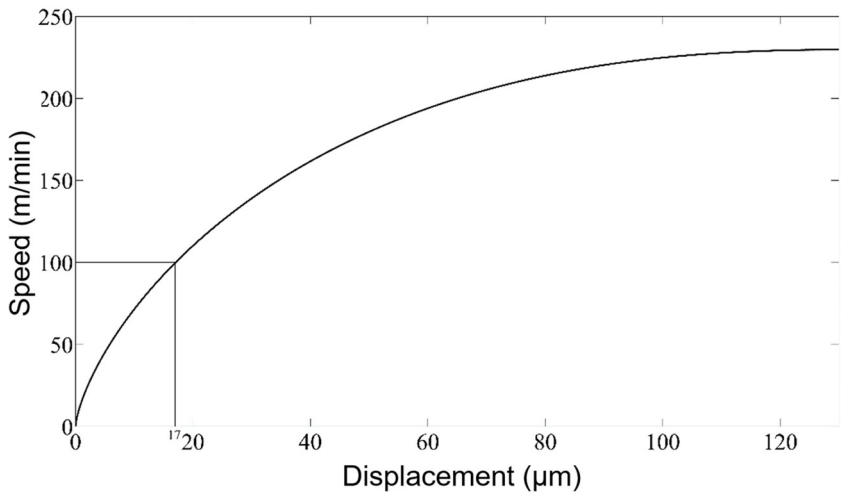


**Fig. 5** Carriage displacement during separation

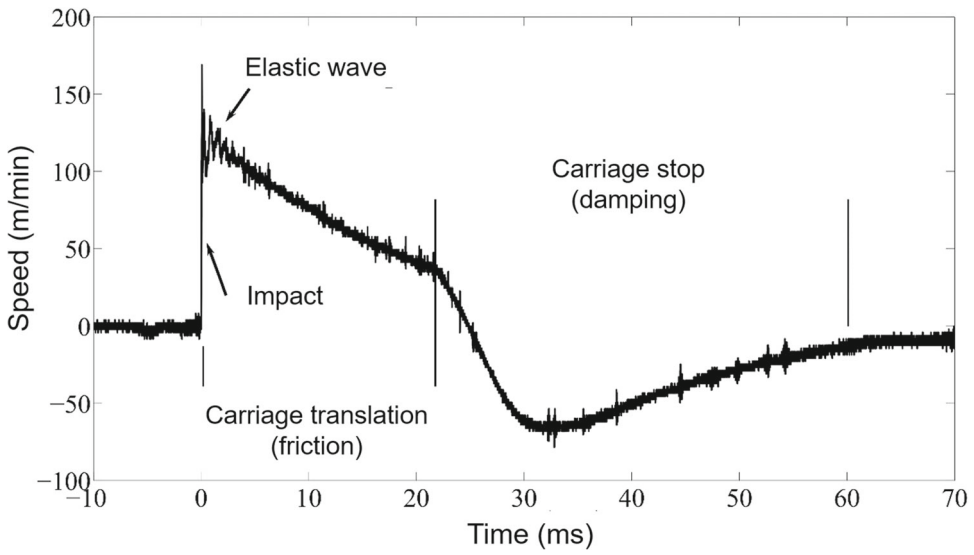


**Fig. 6** Carriage speed during quick-stop test

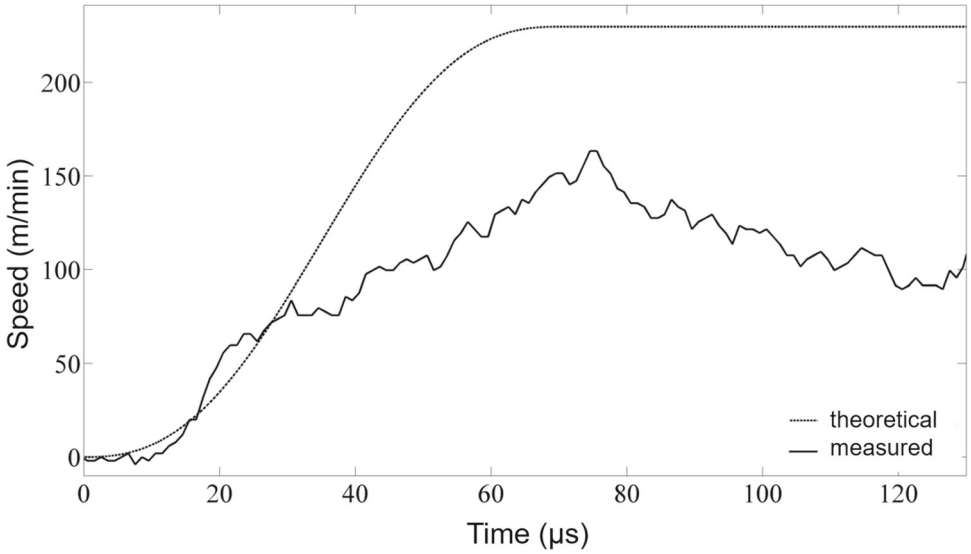


**Fig. 7** Carriage speed during quick-stop test

$t_+$ (Eq. 31), the duration of the percussion can be deduced (Eq. 32).

$$\int_{t^*}^{t_+} dt = t_+ - t^* = -\frac{\delta_{max}}{(V\,(t_+, S_2/R) - V\,(t_+, S_1/R))} \times \int_1^0 \frac{d\Delta}{\sqrt{1-\Delta^{\frac{5}{2}}}} \tag{31}$$

$$\int_{t_-}^{t^*} dt = t^* - t_- = \frac{\delta_{max}}{(V\,(t_+, S_2/R) - V\,(t_+, S_1/R))} \times \int_0^1 \frac{d\Delta}{\sqrt{1-\Delta^{\frac{5}{2}}}} \tag{30}$$

$$t_+ - t_- = \frac{\delta_{max}}{(V\,(t_+, S_2/R) - V\,(t_+, S_1/R))} \times 2,94 \tag{32}$$

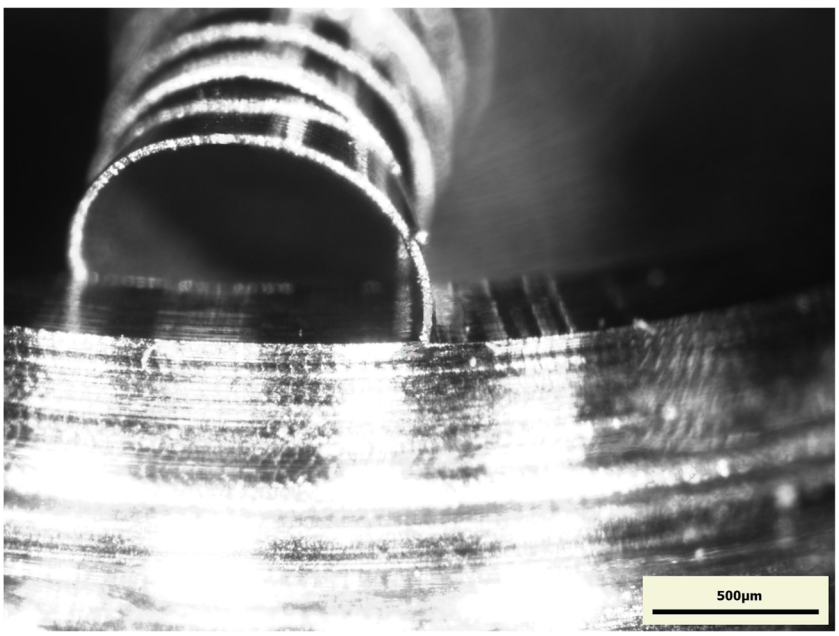


**Fig. 8** Interrupted chip obtained

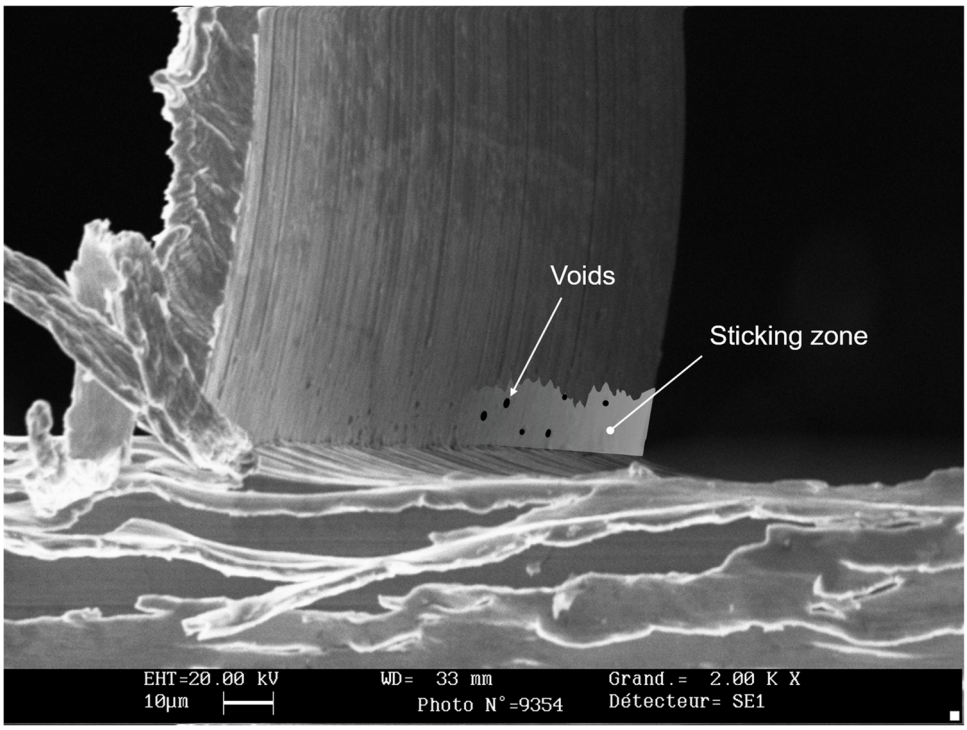


**Fig. 9** SEM observation of chip root

## 3 Results

### 3.1 Theoretical results

The Table 1 gives the characteristics of the QSD. The maximum ejection velocity of the carriage is 230 m/min which is twice as high as the limiting velocity of the study.

The Figs. 4 and 5 allow to observe carriage motion as a function of time from the contact and the displacement given by the non-linear differential Eq. 23. It can be seen that the ejection velocity reaches 100 m/min after a displacement of 17 $\mu$m corresponding to a duration of 32.5 $\mu$s. However, the curve does not take into account the force due to the permanent magnet and the cutting forces, which are neglected.

### 3.2 Measurement of carriage motion

A measurement with a laser vibrometer with sufficient characteristics compared to the theoretical limits allowed the system to be validated. Several remarks should be made. The first concerns the translational guidance by means of ball rails, which introduces friction during the movement of the carriage. It can be seen on the Fig. 6. The effect of this friction decreasing the ejection speed over time. As the tool is largely free on this part, this problem is not critical in the system and rigidity is favoured.

The second concerns the impact, where the measured characteristics are different from the theoretical ones. The comparison of the velocities at impact is given in the Fig. 7 where a difference in achieved velocity can be observed. The ejection speed of the piston was measured and is identical to the theoretical value. The lower than expected ejection velocity of the carriage is the result of absorbed energy that was not taken into account and can also explain the appearance of an elastic wave on the velocity profile. Several possibilities are considered: the damping effect of the air in the impact system or the geometry of the impact interface. It is proposed to increase the number of air channels.

### 3.3 Quick-stop test

Quick-stop test with a cutting speed of 50 m/min were carried out on a rigid machine Röders RP600. The machine table has only one translation axis, the other two being obtained by the movement of the spindle. The device was positioned to have a displacement direction orthogonal to the translation axis in order to reach a high rigidity during the test. In the end, the chips obtained seem to be consistent with expectation (Fig. 8).

The forming chip was observed by SEM. The Fig. 9 shows an area at the base of the chip with voids and free of marks of sliding caused by the chip rubbing against the tool. The possibility of the material sticking to the cutting edge is favoured. A slight rise in the machined surface can also be observed. This can be explained by the clearance angle given to the device. It is suggested to reduce this angle.

## 4 Conclusion

In this work, the development of a quick-stop device dedicated to micro-cutting is presented. The characteristic of this bench is the use of a permanent magnet holding system due to the low cutting forces. The ejection speed and the separation time of the carriage are defined and allow to ensure the efficiency of the device at micro-machining cutting conditions (cutting speed lower than 100 m/min and uncut chip thickness in micron range). However, some elements need to be improved:

- the evacuation of air in the impact system to avoid damping on impact,
- the exhaust angle is too large to avoid undercutting which can disrupt the formation of the chip at the moment of impact.

It should be noted, however, that the device allows "frozen" chip formation to be obtained and the contact zones between the tool and the chip to be observed.

**Acknowledgements** This work was developed in the context of the Manufacturing'21 research group gathering 21 french laboratories in the field of advanced manufacturing.

**Author contribution** All authors contributed to the study conception and design, material preparation, data collection and analysis. The first draft of the manuscript was written by the corresponding author and all authors commented on previous versions of the manuscript. All authors read and approved the final manuscript.

## Declarations

**Conflicts of interest** The authors wish to acknowledge the french Ministère de l'Enseignement Supérieur, de la Recherche et de l'Innovation (MESRI) for the financial support. The authors have no relevant financial or non-financial interests to disclose.

## References

1. Balázs BZ, Geier N, Takács M, Davim JP (2021) A review on micro-milling: recent advances and future trends. Int J Adv Manuf Technol 112(3):655–684. https://doi.org/10.1007/s00170-020-06445-w
2. Chen N, Li HN, Wu J, Li Z, Li L, Liu G, He N (2021) Advances in micro milling: from tool fabrication to process outcomes. Int J Mach Tool Manuf 160. https://doi.org/10.1016/j.ijmachtools.2020.103670
3. Piquard R, Thibaud S, D'Acunto A, Fontaine M, Dudzinski D (2017) Phenomenological modelling of micro-cutting based on experimental results. Int J Adv Manuf Technol 88(9):3429–3436. https://doi.org/10.1007/s00170-016-9047-9
4. Chaabani L, Piquard R, Abnay R, Fontaine M, Gilbin A, Picart P, Thibaud S, D'acunto A, Dudzinski D (2022) Study of the influence of cutting edge on micro cutting of hardened steel using FE and SPH modeling. Micromachines 13(7):1079. https://doi.org/10.3390/mi13071079
5. Rebaioli L (2012) Design and characterization of a new quick-stop device for micromachining
6. Satheesha M, Jain V, Kumar P (1990) Design and development of a quick-stop device (QSD). Precis Eng 12(4):205–212. https://doi.org/10.1016/0141-6359(90)90062-4
7. Ellis J, Kirk R, Barrow G (1969) The development of a quick-stop device for metal cutting research. Int J Mach Tool Des Res 9(3):321–339. https://doi.org/10.1016/0020-7357(69)90007-9
8. Schneider F, Bohley M, Lohkamp R, Sousa F, Müller R, Aurich J (2014) Development of a quick-stop-device to investigate chip formation in micro-and nanomachining
9. Schneider F, Bischof R, Kirsch B, Kuhn C, Müller R, Aurich J (2016) Investigation of chip formation and surface integrity when micro-cutting cp-titanium with ultra-fine grain cemented carbide. Procedia CIRP 45:115–118. https://doi.org/10.1016/j.procir.2016.02.257
10. Subbiah S, Melkote SN (2008) Effect of finite edge radius on ductile fracture ahead of the cutting tool edge in micro-cutting of al2024-t3. Mater Sci Eng A 474(1–2):283–300. https://doi.org/10.1016/j.msea.2007.04.116
11. Uysal A, Altan E (2015) Effect of ploughing force on cutting forces in micro-cutting with a rounded-edge cutting tool. Mater Today: Proceed 2(1):224–229. https://doi.org/10.1016/j.matpr.2015.04.026